SAND2015-7242C

New insights gained on mechanisms of low-energy proton-induced SEUs by minimizing energy straggle

N. A. Dodds, P. E. Dodd, M. R. Shaneyfelt, F. W. Sexton, M. J. Martinez, J. D. Black, P. W. Marshall, R. A. Reed, M. W. McCurdy, R. A. Weller, J. A. Pellish, K. P. Rodbell, and M. S. Gordon

***Abstract*— We present low-energy proton SEU data on a 65 nm SOI SRAM whose substrate has been completely removed. Since the protons only had to penetrate a very thin buried oxide layer, these measurements were affected by far less energy loss, energy straggle, flux attrition, and angular scattering than previous datasets. The minimization of these common sources of experimental interference allows more direct interpretation of the data and deeper insight into SEU mechanisms. The results show a strong angular dependence, demonstrate that energy straggle, flux attrition, and angular scattering affect the measured SEU cross sections, and prove that proton direct ionization is the dominant mechanism for low-energy proton-induced SEUs in these circuits.**

***Index Terms*—single-event effects, low-energy protons, proton direct ionization, soft error rate prediction.**

I. Introduction

For older integrated circuit (IC) technologies, protons could only cause single-event upsets (SEUs) through nuclear interactions, which occur at high proton energies. Recently, large SEU cross sections have been reported from low-energy proton (LEP) irradiations of modern ICs [1]–[3]. These studies present compelling evidence that these upsets are caused by a different mechanism: proton direct ionization. Nonetheless, other mechanisms may also contribute to the LEP SEU response. For example, multiple-bit upsets (MBUs) have been observed when irradiating SOI SRAMs with LEPs at normal incidence, which is inconsistent with the proton direct ionization mechanism because of node spacing [4], [5]. It was suggested in [3]–[5] that elastic scattering might be the cause of these MBUs, while [6] goes so far as to assert that elastic scattering dominates over direct ionization for even single-bit upsets (SBUs).

Thus far, insight into the basic mechanisms of LEP effects has been partially obscured by the interactions of the proton beam with the ICs' intervening materials. Protons are most ionizing when their energy is near 50 keV, at which energy they have a range of only 500 nm in silicon. Even the thinnest of back-end-of-line stacks or thinned substrates are much thicker than this, requiring that higher-energy proton beams be used to penetrate through to the active region. As these protons propagate through the intervening materials their energies are not only degraded, but they also become more broadly distributed: a phenomenon known as energy straggling. Since LEP effects are most significant at very low energies, by the time the beam is degraded to these low energies a fraction of the beam is often stopped altogether, which we will call flux attrition. Finally, as monodirectional protons propagate through the IC materials they scatter off of the target atoms at various angles.

Therefore, when an IC is irradiated with monoenergetic and monodirectional LEPs, what actually reaches the sensitive volumes is a reduced flux of protons at various energies and angles, making it difficult to correctly interpret the resulting SEU cross section. These uncertainties are amplified when increasing the angle of the beam, which effectively increases the thickness of the intervening materials, or when testing circuits in flip-chip packages, which must be irradiated through silicon substrates that usually cannot be thinned to less than 50 μm.

In this work, we present low-energy proton and alpha particle SEU data for a 65 nm silicon-on-insulator (SOI) SRAM whose silicon substrate has been completely removed. Thus, particles only have to penetrate the 150 nm thick buried oxide (BOX) to reach the sensitive volumes. In previous studies, the intervening materials were at least 10 μm thick, or about 70 times thicker. (One exception is [7], in which these same SRAMs were also tested with LEPs through the BOX. However, tests were only performed at normal incidence over a narrow range of energies due to facility constraints.) Therefore, energy loss, energy straggle, flux attrition, and angular scattering have been dramatically reduced in this work. This allows the LEP energy and angular responses to be studied independently for the first time, and provides more direct insight into the roles of these parameters than was possible in previous studies. The results prove that proton direct ionization is the dominant mechanism for LEP-induced SEUs in these circuits. Insights are also gained on angular scattering effects. Finally, methods and assumptions that have been used for LEP error rate prediction are tested and validated.

II. Experimental Details

Low-energy broadbeam irradiations were performed using three accelerators: Vanderbilt University's Pelletron [8], NASA Goddard's Instrument Calibration Van de Graaff [9], and NASA Goddard's Potential Drop Accelerator [9]. The beam flux was uniform across the spot size, which was 1,

Manuscript received July 10, 2015. This work was supported by the Laboratory Directed Research and Development program at Sandia National Laboratories, a multi-program laboratory operated by Sandia Corporation, a Lockheed Martin Company, for the United States Department of Energy, under contract DE-AC04-94AL85000.

N. A. Dodds, P. E. Dodd, M. R. Shaneyfelt, F. W. Sexton, M. J. Martinez, and J. D. Black are with Sandia National Laboratories, Albuquerque, NM 87123 USA (email: nadodds@sandia.gov).

P. W. Marshall is an NRL consultant from Brookneal, VA 24528 USA.

R. A. Reed, M. W. McCurdy, and R. A. Weller are with Vanderbilt University, Nashville, TN 37203 USA.

J. A. Pellish is with NASA Goddard Space Flight Center, Greenbelt, MD 20771 USA.

K. P. Rodbell and M. S. Gordon are with the IBM T.J. Watson Research Center, Yorktown Heights, NY 10598 USA.

0.63, and 0.5 inches for these three accelerators, respectively. Highly monoenergetic beams were used and maintained by testing in vacuum and by tuning the accelerators to the energy of interest. With only one exception (discussed later), degraders were not used to reduce the beam energy. The beams were verified to be pure by measuring their energy distributions with surface barrier detectors, which were placed behind apertures with very small openings, and which were calibrated using an Am-241 source. Finally, rotation stages in the vacuum chambers allowed the tilt angle of the IC to be controlled remotely.

Vanderbilt's Pelletron was tuned to produce 0.25 to 4 MeV proton beams, and 6 MeV alphas. The uniform 1 inch diameter broadbeam is produced using a 120 nm thick gold scattering foil, located 3.1 meters upstream of the IC being tested. This foil is so thin that it causes negligible energy loss and energy spreading. Rutherford back-scattered particles from this foil are counted to provide dosimetry. This dosimetry system allows the flux at the IC to be reported in real time, without blocking the beam, and is calibrated using a solid-state detector that can be inserted at the IC test position. Most tests were performed in vacuum, but some were also performed in air by passing the beam out of a 25.4 μm thick aramica exit window.

The two NASA accelerators were tuned to produce proton beams from 25 to 250 keV. On these accelerators, the flux was uniform across the spot size because of how the beam diverges from the upstream bending magnets. No scattering foils were necessary. The beam flux was measured immediately before and after each irradiation of the IC. For the Van de Graaff, this was done with a beam stop electrode that was calibrated with a Faraday cup, while for the Potential Drop Accelerator, this was done with an apertured surface barrier detector that was calibrated with a Faraday cup.

All tests were performed at ambient temperature on partially-depleted SOI SRAMs made in IBM's 65 nm technology node. SRAMs of this same model were tested with LEPs in [1], [2], [4], [7]. Bias voltages of 0.8 V and 1.0 V were used, corresponding to undervoltages of approximately 30% and 10%, respectively. A Certimax digital tester was used to write (read) a checkerboard pattern to (from) the SRAMs before (after) each irradiation.

The SRAMs' substrates were completely removed using the XeF_2 etch process described in [10], [11]. All irradiations were performed through the backside, so the particles only had to pass through the 150 nm thick BOX to reach the sensitive volumes. Even when following best practices, this etching process leaves islands of some residual material on the BOX [11]. Recent work has shown that these are islands of SiO_x, which are formed during the etch process [12]. After the radiation tests were complete, the islands on the SRAMs' buried oxides were studied using optical, scanning electron, and atomic force microscopes. These showed that the SiO_x islands were less than 10 nm thick—far thinner than the 150 nm thick buried oxide. Therefore, these islands are assumed to have a negligible effect on the beams used.

Tests were performed at angles of up to 80°. The SRAMs' packages were specially prepared to allow testing at this angle without obstructing the beam. At these extreme angles, small uncertainties in the beam angle can significantly affect the SEU cross sections. This uncertainty was minimized by re-zeroing the rotation stages at angles that caused the same cross sections to be measured at +80° and -80°.

III. Results With Significant Energy Loss and Energy Straggle

The measurements of Fig. 1 demonstrate how LEP measurements are typically performed. Typically, energy loss and straggle are significant, and degraders are often used to decrease the beam energy, as was done in [2]–[5]. It is well known that these degraders introduce uncertainty in the measurements via energy straggle. Despite this, degraders are still used, either of necessity since some accelerators cannot be tuned to low enough energies, or of convenience to avoid the delays imposed by retuning the accelerator. For Fig. 1, irradiations were performed at Vanderbilt using normally-incident 4 MeV protons in air. In this case, the air gap was increased to degrade the beam energy. The measurements of Fig. 1 (and of all measurements performed in this work) are plotted with error bars that represent the 95% confidence interval, based on the number of SEUs observed. If error bars are not visible for a given datapoint, then they are smaller than that point. A peak cross section was observed when an air gap of 21 cm was used, because that air gap caused many of the protons to reach the sensitive volumes near their end of range, where their linear energy transfer (LET) is highest. It is expected that a larger peak cross section would be measured if monoenergetic protons could be delivered to the sensitive volumes near their end of range, which will be confirmed in the next section.

Data were gathered in a similar manner in [2], and are presented in Fig. 2. In this case, irradiations were performed in vacuum with 1 MeV protons through the back-end-of-line (BEOL) materials. The BEOL is ~10 μm thick for this technology [2]. The beam angle was increased, which effectively increased the thickness of the BEOL degrader materials. The peak cross section occurred at 50° because, at that angle, the BEOL had an effective thickness of ~16 μm, which is also the range of 1 MeV protons in silicon. In other words, the peak occurred at 50° because, at that angle, the BEOL materials degraded the protons so that they reached

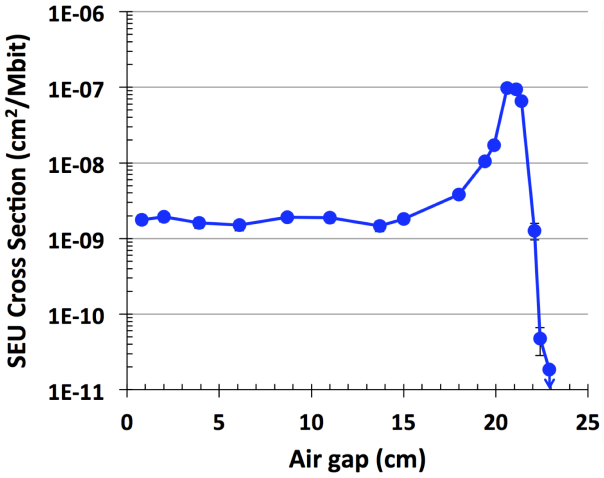

Fig. 1. Measured SEU cross sections for normally-incident 4 MeV protons as a function of air gap thickness at 0.8 V.

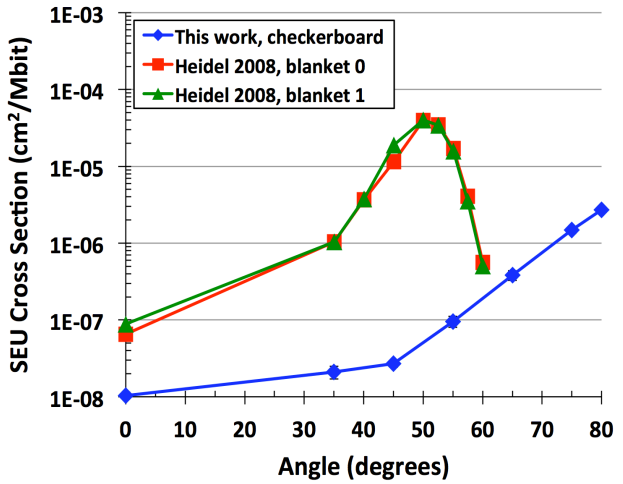

Fig. 2. Measured SEU cross sections as a function of beam angle for 1 MeV protons in a vacuum on the IBM 65 nm SOI SRAMs biased to 1.0 V. The cross sections differ because of differences in energy loss, energy straggle, and flux attrition, which were significant in [2], but which were insignificant in this work.

the sensitive volumes near their end of range, where their LET is highest. This is why these data are qualitatively similar to those of Fig. 1. (Note that the BEOL isn't composed entirely of Si, but the average density of all the BEOL materials is similar to that of Si.)

This peak cross section that occurred at 50° was used in [2] for an on-orbit error rate calculation. Similarly, peak cross sections measured in [13] were used for LEP error rate calculations. These studies used these peak cross sections, even though they were known to be affected by energy straggle and flux attrition, because at that time it was not possible to further reduce these sources of experimental interference. Thus, energy straggle and flux attrition introduced uncertainty into these error rate calculations that was not quantified.

IV. Insights Gained When Minimizing Energy Loss and Energy Straggle

The blue curve of Fig. 2 was measured using the same proton energy (1 MeV), SRAM model, and bias voltage as the other Fig. 2 curves that were taken from [2]. However, the resulting cross sections are very different because of differences in energy loss, energy straggle, and flux attrition, which were significant in the measurements of [2] due to the relatively thick BEOL materials, but which were insignificant in this work since the protons only had to penetrate the 150 nm thick buried oxide. These differences demonstrate that experimental results should be interpreted cautiously when the energy loss and straggle in intervening materials are significant.

The cross sections of the blue curve of Fig. 2 increase with angle due to the increase in effective LET of the proton direct ionization. In other words, the protons have a longer path length through the sensitive volumes at the larger angles, thereby depositing more charge and making SEUs more likely. Note that the cross sections of Fig. 2 are not scaled by 1/cos(angle) to account for the lower flux reaching the SRAM at the larger angles. If they were, then the cross section at 60° would be 2× higher, and the cross section at 80° would be 5.8× higher. Thus, the angular response of this

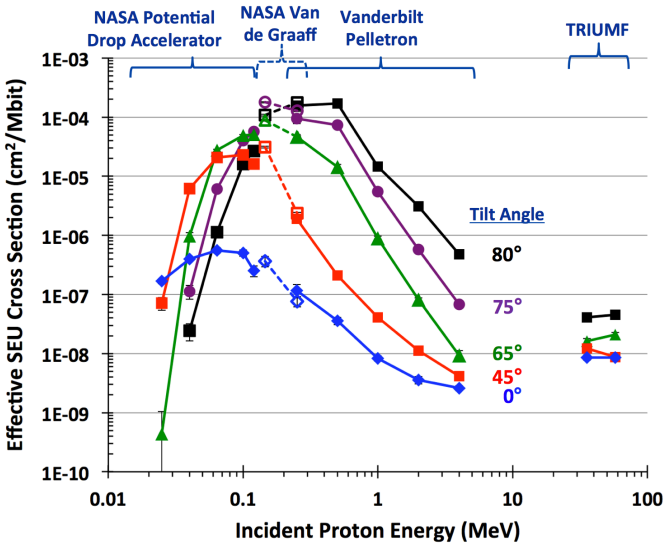

Fig. 3. Measured proton SEU cross sections using four accelerators, angles of 0-80°, incident energies of 25 keV to 58 MeV, and a bias of 0.8 V. These data were affected by far less energy loss, energy straggle, angular scattering, and flux attrition than data from previous studies because only 150 nm of intervening IC material (SiO_2) was present.

SRAM is even stronger than is suggested by the blue curve. In the curves from [2], the angle, average energy, energy straggle, and flux of the protons reaching the sensitive volumes were all changing together, and their separate roles cannot be decoupled. Conversely, only the angle of the protons is changing in the blue curve, since energy loss, energy straggle, and flux attrition in the BOX is negligible.

The complete dataset in which energy loss, straggle, and flux attrition have been minimized is shown in Fig. 3. Four different accelerators were used, spanning incident proton energies of 0.025 to 58 MeV. The accelerators used for each energy range are labeled at the top of Fig. 3. The results obtained at TRIUMF are from [7]. The same 65 nm SRAM sample was used for the TRIUMF and Pelletron datasets. This sample was subsequently damaged, so a different sample had to be used for the NASA datasets. It can be seen that the same cross sections were measured from these two samples at 0.25 MeV with the Pelletron and NASA Van de Graaff, so the results from these two samples are treated as a single data set.

Irradiations were performed using *tilt* angles of 0-80°, where *tilt angle* has the usual meaning of the angle between the incident protons and the normal to the plane of the IC surface. The *roll* angle (rotation of the IC with respect to the incident particle trajectory) was chosen so that grazing angle protons traveled along the transistor gates, or more importantly, through the long dimension of the transistors' body and channel regions. If the SEU cross sections depend on the roll angle then this is expected to be the worst-case roll angle. However, LEP results from [7] on these same SRAMs showed that the SEU cross section did not depend on the roll angle for the conditions used therein.

The data of Fig. 3 are plotted as *effective* SEU cross sections, meaning they have been scaled by 1/cos(angle) to account for the reduction in flux as the angle is increased. This is typically done with SEU data caused by *heavy ion* direct ionization, and is done here since the SEUs from 0.025

to 4 MeV were caused by *proton* direct ionization. However, the TRIUMF data at 36 and 58 MeV were caused instead by proton nuclear interactions. If these TRIUMF cross sections had not been scaled by 1/cos(angle) then they would be seen to be equal from 0-80°, as is typical of data caused by proton nuclear interactions.

Fig. 3 shows a strong energy response. The SEU cross sections are a few orders of magnitude higher at low energies than they are at 58 MeV, consistent with the findings of previous works [2], [3], [13]. However, previous works could not show the energy response at this level of detail because the ICs had much thicker intervening materials. Fig. 3 shows that SEUs were observed with incident proton energies as low as 25 keV. To the knowledge of the authors, these are the lowest energy particles that have ever been observed to cause SEUs. More importantly, the maximum cross section at 0° was measured at 64 keV. This is very close to the proton Bragg peak energy of ~50 keV, which is the energy at which protons are the most ionizing. Therefore, this energy has always been expected to be the worst-case energy for proton direct ionization-induced SEUs, at least in circuits with very thin sensitive volumes such as this one, but this has not been experimentally verified until now. This is compelling evidence that direct ionization is the dominant mechanism for LEP-induced SEUs, at least in this circuit. Note that the Bragg peak energy for protons is not well defined [14], so the maximum SEU cross section was not expected to be at exactly 50 keV.

It is instructive to compare the peak cross sections measured at 0° in Figs. 1 and 3. Both measurements were made with a bias voltage of 0.8 V. The difference is that 4 MeV protons were degraded until a peak cross section was found in Fig. 1, whereas in Fig. 3 the proton beams were directly tuned to find the peak cross section. The peak cross sections in Figs. 1 and 3 are ~1 × 10^{-7} cm^2/Mbit and ~6 × 10^{-7} cm^2/Mbit, respectively. Therefore, the peak cross section measured with a degraded beam was ~6× lower than that measured with a monoenergetic beam. Radiation transport simulations performed with MRED [15], [16] and SRIM [17] (not presented) suggest that the 0° peak cross section was lower in Fig. 1 than in Fig. 3 because energy straggle, flux attrition, and angular scattering were significant in Fig. 1, which prevented most protons from reaching the sensitive volumes at their worst-case energy of ~50 keV, as they did in Fig. 3. (The simulations suggest that energy straggle and flux attrition were more significant factors than angular scattering.) This suggests that energy straggle and flux attrition cause the peak cross sections of conventional LEP measurements to be lower than they would be otherwise, so those measurements are not conservative and should be interpreted cautiously.

Fig. 3 also shows a strong angular response. From 0.15 to 4 MeV, the cross sections increase by 2-4 orders of magnitude as the angle is increased from 0° to 80°. This demonstrates more convincingly than previous studies that one must account for the LEP angular response to be conservative. Most LEP test methods are not amenable to testing at grazing angles since that worsens energy straggle in the intervening materials. One exception is presented in [7], in which energy straggle is intentionally introduced to reproduce the LEP distribution found in space. Although grazing angles were found to be the worst case for LEPs in SOI SRAMs in this study and in [7], [18], results from [18] suggest that bulk Si ICs have a very different LEP angular response, and that the worst-case angle is at or near normal incidence.

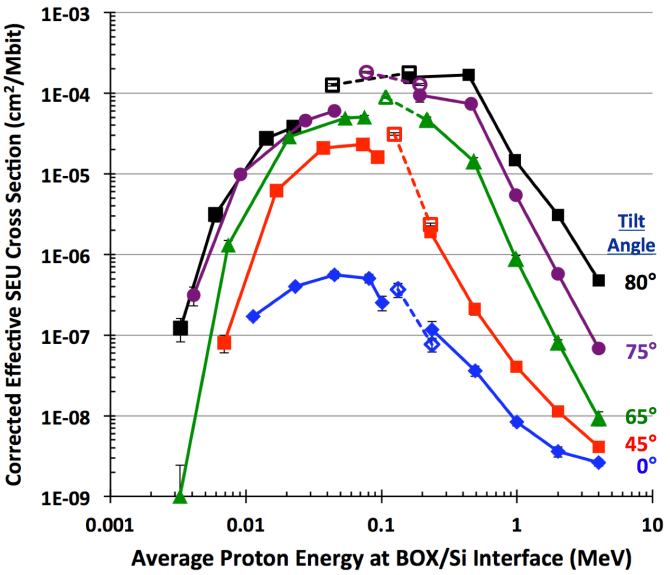

Fig. 4. Measured proton SEU cross sections from Fig. 3, replotted as a function of average proton energy at the buried oxide/silicon interface, and corrected for the minor flux attrition that occurred in the buried oxide. These adjustments were made based on SRIM simulation results.

The low-energy data of Fig. 3 have been replotted in Fig. 4. The cross sections have been corrected based on SRIM simulation results to compensate for the minor flux attrition that occurred in the BOX. More importantly, SRIM simulation results were used to account for energy loss in the BOX by replotting the data as a function of average proton energy at the BOX/Si interface, which is the top surface of the sensitive volumes. Both of these changes primarily altered the data taken at the lowest incident energies and largest angles, on which even the very thin BOX had a non-negligible effect. For example, when the Fig. 3 datapoint at 80° and 40 keV was replotted to account for energy loss in the BOX, it shifted down to ~3 keV in Fig. 4; a larger shift than was seen for the other angles.

The LEP data of Fig. 3 have also been replotted in Fig. 5, except in this case they are plotted as a function of the average effective LET at the BOX/Si interface based on SRIM simulation results. Effective LET is the LET at normal incidence times 1/cos(angle). In Fig. 5a, the proton data gathered at incident energies of 0.25-4 MeV are plotted along with 6 MeV alpha particle data gathered with the Vanderbilt University (VU) Pelletron from 0-80°, and along with heavy ion data reported by Heidel *et al.* in [4]. Heidel's data were gathered at TAMU using 40 MeV/u N and 15 MeV/u Ne at the same bias voltage (0.8 V) on the same model SRAM, but it was irradiated through the BEOL and its substrate was not removed. The excellent agreement of the proton and alpha data of this work with the green datapoints from [4] suggest that the SRAM's intrinsic SEU susceptibility was not altered when the substrate was removed, consistent with the findings of [19].

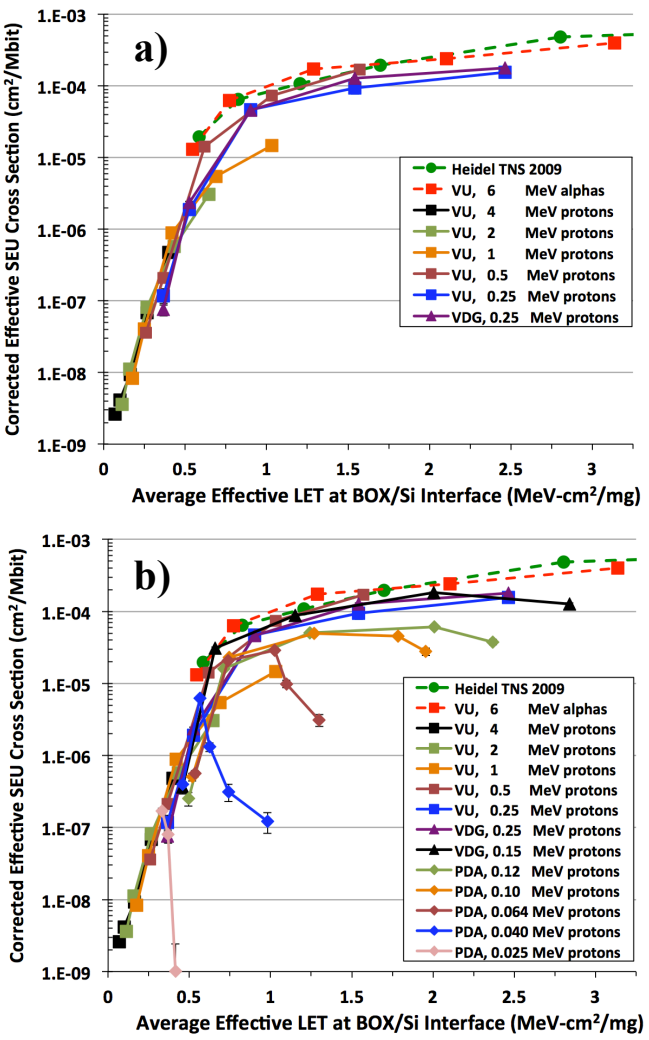

Fig. 5. Measured proton SEU cross sections from Fig. 3, replotted as a function of average effective LET at the buried oxide/silicon interface, and corrected for the minor flux attrition that occurred in the buried oxide. These adjustments were made based on SRIM simulation results. The data are plotted down to incident proton energies of a) 0.25 MeV and b) 0.025 MeV, and show a) good agreement with a Weibull-shaped curve which also includes data taken with alphas and heavier ions, and b) divergence from the Weibull-shaped curve.

Nearly all the datapoints of Fig. 5a fall along the same Weibull-shaped curve, even though a very wide range of particle species, angles, and energies were used. The highest LET (highest angle) datapoint for 1 MeV protons is an outlier, which is not understood at this time. This agreement between the proton, alpha, and heavier ion data suggests that effective LET in the sensitive volume is sufficient to predict SEU cross sections. This proves that direct ionization is the dominant LEP SEU mechanism, at least for SBUs in this circuit (no MBU analysis is performed in this work). In spite of this finding, at this time we recommend that low-LET ions (such as alphas) not be used as a proxy for LEP testing since these low-LET ions have been shown to underpredict the cross sections for LEP-induced MBUs [5]. Further work is needed to understand the mechanism for these LEP-induced MBUs so that hardness assurance guidelines can be adjusted accordingly.

In contrast to Fig. 5a, Fig. 5b shows that the effective LET metric has its limits. Fig. 5b contains the same data as Fig. 5a, as well as the proton data gathered with incident energies of 0.025-0.15 MeV. These lower-energy data diverge from the Weibull-shaped curve, especially as the angle (and effective LET) is increased and as the incident proton energy is reduced. SRIM simulations were performed that indicate this occurs because, although the protons *enter* the sensitive volumes with the effective LET shown on the X-axis, their effective LET is much lower when they *leave* the sensitive volumes, if they leave the sensitive volumes at all. For example, consider the datapoint measured with an initial energy of 40 keV at 80°, which has the highest effective LET of this data series. By the time this beam penetrates the BOX it has an average energy of only ~3 keV, as shown in Fig. 4. SRIM reports that 3 keV protons have an average range of ~50 nm in Si. The SRAM's sensitive volumes are ~60 nm thick, which is the Si film thickness for this SOI technology [20]. At an angle of 80°, the path length through this ~60 nm thick sensitive volume is ~350 nm, which is much greater than the ~50 nm range of the 3 keV protons. In other words, the datapoints that diverge from the main curve in Fig. 5b do so because the proton energies are too low to maintain their effective LETs all the way through the sensitive volumes. Therefore, if the sensitive volumes had been thicker, as is the case with bulk Si circuits, then this divergence from the main curve would have been more significant.

V. Angular Scattering Effects

The role of angular scattering was minimized in the data of Figs. 3-5 since the SRAMs' intervening materials were reduced to only 150 nm of SiO_2. However, even under these nearly ideal experimental conditions, angular scattering still affected the measurements, as will now be shown using SRIM simulations.

Simulations were performed of monoenergetic proton beams with energies ranging from 25 to 250 keV, corresponding to the test energies used with the two NASA accelerators. One million protons were simulated in each case, and were directed at a 150 nm thick layer of SiO_2, representing the buried oxide of the etched SOI SRAM. For those protons that were transmitted through the oxide, the angles at which they were emitted were recorded and histogrammed in 1-degree-wide bins. These histograms give insight into the angular distributions of protons reaching the sensitive volumes in the experiments of Figs. 3-5.

Fig. 6 shows the angular distributions from simulations performed with protons at a 65° angle. The X-axis is plotted as the *departure* from this 65° angle, in degrees. Therefore, if the beam were to pass through the BOX without scattering, then all one million counts would be plotted at zero degrees on the X-axis. Instead, we see semi-Gaussian distributions, which become increasingly broad as the initial energy is reduced from 250 to 25 keV. This demonstrates that scattering effects are most severe at very low energies. Therefore, although proton irradiations were performed with monodirectional beams at certain angles in Figs. 3-4, the protons reaching the sensitive volumes had angular distributions, which were most broad at the lowest energies.

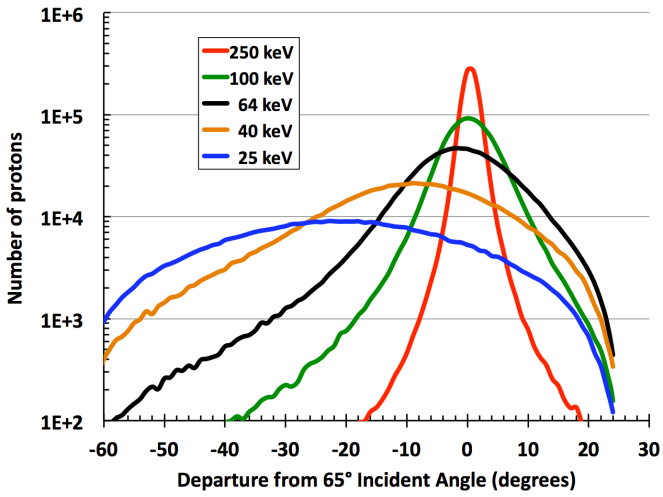

Fig. 6. SRIM simulation results of 65° tilted proton beams of five different initial energies after having passed through the 150 nm thick buried oxide. This angular histogram shows that, as their initial energy is reduced, protons are more likely to scatter at large angles. Also, at an initial energy of 25 keV, most protons that are transmitted through the BOX are able to do so because scattering causes them to have shorter path lengths through the BOX, which corresponds to negative angles on the X-axis.

Fig. 6 also shows that the peaks of the angular distributions shifted to large negative angles as the initial beam energy was reduced. Note that negative angles correspond to protons traveling through the BOX with a shorter path length. Therefore, the 25 keV beam scattered at many angles upon striking the BOX, and those protons that scattered at large negative angles were most likely to be transmitted all the way through the BOX because of their shorter path lengths. The conditions used for this simulation result—65° with an initial energy of 25 keV—were also used experimentally for one datapoint in Fig. 3. This measured cross section is seen to be very low, and would likely have been even lower in the absence of scattering. Thus, scattering can affect not only the angle and the effective LET of the protons that reach the sensitive volumes, but can also affect the energy loss, energy straggle, and flux attrition occurring in the intervening materials. More detailed simulations would be necessary to quantify the effect of scattering on the measured cross sections of Fig. 3. However, the good agreement of the datapoints of Fig. 5a with the Weibull-shaped curve suggest that scattering had very little effect on the cross sections measured with those beams, whose incident energies were 250 keV or more. This is consistent with Fig. 6, which shows that a 250 keV proton beam undergoes very little angular scattering in the 150 nm thick BOX.

It is expected that scattering effects will be more severe when the intervening materials are thicker than the 150 nm BOX of this study, which has always been the case in prior LEP experiments. Therefore, scattering effects require further investigation, especially since they may have caused the MBUs that were observed when irradiating SOI SRAMs with LEPs at normal incidence in [4], [5].

VI. Insights Gained on LEP Error Rate Prediction

The technique used in this work to minimize energy loss, energy straggle, flux attrition, and angular scattering has proven useful for understanding LEP mechanisms, but is not very practical for routine hardness assurance applications. Its use is limited to SOI circuits, and it imposes strenuous circuit preparation and facility requirements. It is the opinion of the authors that the most practical error rate prediction method for LEPs is the one developed in [7], [18]. This method was developed using the same 65 nm SOI SRAM and 0.8 V bias voltage used in this work. Therefore, the nearly monoenergetic data of this work can be used to test the accuracy of that method, and the validity of one assumption on which it relies.

The LEP rate prediction method of [7], [18] intentionally introduces significant energy straggle by degrading a 70 MeV proton beam. Energy spectroscopy measurements and simulations were used to show that, by so doing, the LEP energy distribution found in all shielded space environments could be reproduced in the laboratory. The beam is degraded until the peak SEU cross section from LEPs is found. This peak cross section is caused by a space-like LEP energy distribution that is delivered to the sensitive volumes with a known fluence. This dramatically simplifies LEP error rate prediction, and allows work to be done at high-energy proton facilities, on encapsulated parts, without knowledge of the IC design, and with no computer simulations required [7], [18].

To test the accuracy of this method, LEP error rate predictions were performed using the data of Fig. 3 for the same space environments for which error rates were predicted in [7]. The steps of this error rate calculation are as follows:

1. The Fig. 3 data from 0.025-4 MeV and 0-80° were interpolated to produce cross sections at the same proton energies listed in the environments' differential flux files.
2. Each of these cross sections was multiplied by the differential flux at the corresponding energy, and by the width of that energy bin in the flux file.
3. These fractional error rates were integrated from 0-3 MeV, giving the error rates based on data at each of the five angles shown in Fig. 3.
4. These integral error rates were weighted according to the probabilities that proton strikes that occurred would occur at or near those angles. The same weighting factors were used that are given in Table I of [7].
5. These weighted integral error rates were summed together, giving the total error rate to isotropic sub-3-MeV space protons.

For every space environment considered, the error rates calculated using the data of Fig. 3 and the steps above were 50% higher than the error rates calculated in [7]. This is an excellent agreement for error rate calculations, for which small changes in the input parameters can often lead to much larger changes in the calculated error rates. This excellent agreement is surprising since the method of [7] relies on degraded 70 MeV proton beams, whereas the rate calculations of this work used monoenergetic beams. This confirms that the method of [7] is both accurate and practical.

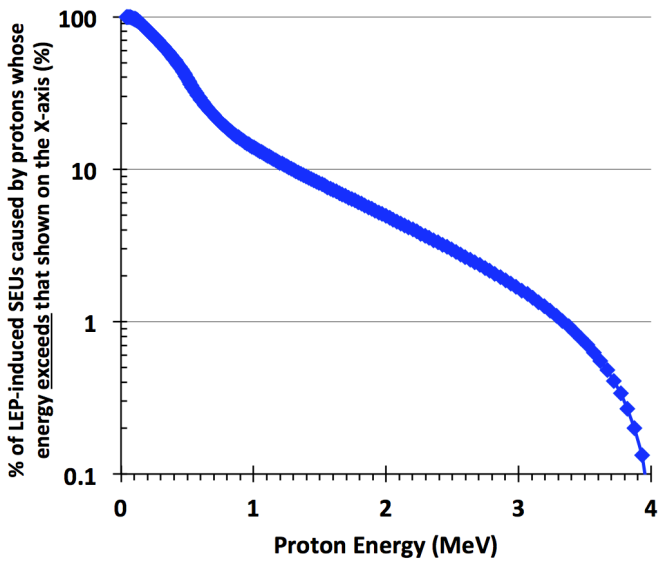

Fig. 7. Integral histogram showing the percentage of LEP-induced SEUs caused by protons whose energy exceeds that shown on the X-axis, for the 65 nm SOI SRAM in a GEO Worst Day Solar Flare environment behind 100 mils Al shielding.

The error rate prediction method of [7] assumed that protons that reach the sensitive volumes with over 3 MeV have a negligible contribution to the total LEP error rate. (Similar assumptions regarding upper energy cutoffs have been made, either explicitly or implicitly, in nearly every work that calculates error rates from LEPs. For one example, see [21].) The fractional error rates calculated in step 2, above, allow this assumption to be tested, at least for LEPs in this 65 nm SOI SRAM.

Fig. 7 was calculated based on the fractional error rates described in the steps above for the 65 nm SOI SRAM in a GEO Worst Day Solar Flare environment behind 100 mils of Al shielding. These fractional error rates were normalized and integrated to allow the data of Fig. 7 to be read as percentages of all LEP-induced SEUs caused by protons whose energies *exceed* those shown on the X-axis. For example, it can be seen that protons with energies > 3 MeV only cause about 2% of LEP-induced errors in this SRAM. This confirms the assumption made in [7] that protons with energies > 3 MeV have a negligible contribution to the total LEP error rate.

VII. Summary

Low-energy proton SEU data are presented in which energy loss, energy straggle, flux attrition, and angular scattering have been minimized by removing the SOI SRAM's silicon substrate. By minimizing these common sources of experimental interference, these data give deeper insight into SEU mechanisms than previous datasets.

Results show that grazing angles are the worst case for LEP-induced SEUs in these SOI circuits. (A different LEP angular response was seen for bulk Si circuits in [18].) Angular scattering is shown to affect the measured LEP cross sections to a small degree, even in these circuits with very thin intervening materials. Effective LET in the sensitive volume is shown to be adequate to predict the SEU cross section, even when using protons, alphas, and heavy ions at many different angles and energies, proving that proton direct ionization is the dominant mechanism for LEP-induced SEUs in these circuits. Finally, the LEP error rate calculation method developed in [7] is shown to be accurate.

VIII. Acknowledgements

The authors would like to thank Steve Brown, Marty Carts, and Alvin Boutte for their assistance with the experiments at NASA Goddard, Marcus Mendenhall, for his assistance preparing for the experiments at Vanderbilt University, Steve Buchner (Naval Research Laboratory), for his helpful discussions, and the DTRA RHM program, for its support.

IX. References

[1] K. P. Rodbell, D. F. Heidel, H. H. K. Tang, M. S. Gordon, P. Oldiges, and C. E. Murray, "Low-Energy Proton-Induced Single-Event-Upsets in 65 nm Node, Silicon-on-Insulator, Latches and Memory Cells," *IEEE Trans. Nucl. Sci.*, vol. 54, no. 6, pp. 2474–2479, Dec. 2007.

[2] D. F. Heidel, P. W. Marshall, K. A. LaBel, J. R. Schwank, K. P. Rodbell, M. C. Hakey, M. D. Berg, P. E. Dodd, M. R. Friendlich, A. D. Phan, C. M. Seidleck, M. R. Shaneyfelt, and M. A. Xapsos, "Low Energy Proton Single-Event-Upset Test Results on 65 nm SOI SRAM," *IEEE Trans. Nucl. Sci.*, vol. 55, no. 6, pp. 3394–3400, Dec. 2008.

[3] B. D. Sierawski, J. A. Pellish, R. A. Reed, R. D. Schrimpf, K. M. Warren, R. A. Weller, M. H. Mendenhall, J. D. Black, A. D. Tipton, M. A. Xapsos, R. C. Baumann, X. Deng, M. J. Campola, M. R. Friendlich, H. S. Kim, A. M. Phan, and C. M. Seidleck, "Impact of Low-Energy Proton Induced Upsets on Test Methods and Rate Predictions," *IEEE Trans. Nucl. Sci.*, vol. 56, no. 6, pp. 3085–3092, Dec. 2009.

[4] D. F. Heidel, P. W. Marshall, J. A. Pellish, K. P. Rodbell, K. A. LaBel, J. R. Schwank, S. E. Rauch, M. C. Hakey, M. D. Berg, C. M. Castaneda, P. E. Dodd, M. R. Friendlich, A. D. Phan, C. M. Seidleck, M. R. Shaneyfelt, and M. A. Xapsos, "Single-Event Upsets and Multiple-Bit Upsets on a 45 nm SOI SRAM," *IEEE Trans. Nucl. Sci.*, vol. 56, no. 6, pp. 3499–3504, Dec. 2009.

[5] J. A. Pellish, P. W. Marshall, K. P. Rodbell, M. S. Gordon, K. A. LaBel, J. R. Schwank, N. A. Dodds, C. M. Castaneda, M. D. Berg, H. S. Kim, A. M. Phan, and C. M. Seidleck, "Criticality of Low-Energy Protons in Single-Event Effects Testing of Highly-Scaled Technologies," *IEEE Trans. Nucl. Sci.*, vol. 61, no. 6, pp. 2896–2903, Dec. 2014.

[6] M. Kosmata, J. Auerhammer, M. Zier, F. Schlaphof, F. Schreiter, and J. von Borany, "Influence of proton elastic scattering on soft error generation of SRAMs," in *RADECS Proceedings*, 2011, pp. 186–190.

[7] N. A. Dodds, J. R. Schwank, M. R. Shaneyfelt, P. E. Dodd, B. L. Doyle, M. Trinczek, E. W. Blackmore, K. P. Rodbell, M. S. Gordon, R. A. Reed, J. A. Pellish, K. A. LaBel, P. W. Marshall, S. E. Swanson, G. Vizkelethy, S. Van Deusen, F. W. Sexton, and M. J. Martinez, "Hardness Assurance for Proton Direct Ionization-Induced SEEs Using a High-Energy Proton Beam," *IEEE Trans. Nucl. Sci.*, vol. 61, no. 6, pp. 2904–2914, Dec. 2014.

[8] M. W. McCurdy, M. H. Mendenhall, R. A. Reed, B. R. Rogers, and R. D. Schrimpf, "Vanderbilt Pelletron - Low Energy Protons and Other Ions for Radiation Effects on Electronics," *Accepted to the 2015 NSREC*.

[9] "Goddard Space Flight Center Radiation Effects Facility, [Online]. Available: http://radhome.gsfc.nasa.gov/radhome/ref/gsfc_ref.html." .

[10] N. Kanyogoro, S. Buchner, D. McMorrow, H. Hughes, M. S. Liu, A. Hurst, and C. Carpasso, "A New Approach for Single-Event Effects Testing With Heavy Ion and Pulsed-Laser Irradiation: CMOS/SOI SRAM Substrate Removal," *IEEE Trans. Nucl. Sci.*, vol. 57, no. 6, pp. 3414–3418, Dec. 2010.

[11] M. R. Shaneyfelt, J. R. Schwank, P. E. Dodd, J. Stevens, G. Vizkelethy, S. E. Swanson, and S. M. Dalton, "SOI Substrate Removal for SEE Characterization: Techniques and Applications," *IEEE Trans. Nucl. Sci.*, vol. 59, no. 4, pp. 1142–1148, Aug. 2012.

[12] J. Sniegowski, Sandia National Laboratories, "private communication." Jun-2015.

[13] E. H. Cannon, M. Cabanas-Holmen, J. Wert, T. Amort, R. Brees, J. Koehn, B. Meaker, and E. Normand, "Heavy Ion, High-Energy, and Low-Energy Proton SEE Sensitivity of 90-nm RHBD SRAMs," *IEEE Trans. Nucl. Sci.*, vol. 57, no. 6, pp. 3493–3499, Dec. 2010.

[14] "Stopping Power for Light and Heavier Ions, [Online]. Available: http://www-nds.iaea.org/stoppinggraphs/stopp_bot.htm." .

[15] R. A. Weller, M. H. Mendenhall, R. A. Reed, R. D. Schrimpf, K. M. Warren, B. D. Sierawski, and L. W. Massengill, "Monte Carlo simulation of single event effects," *IEEE Trans. Nucl. Sci.*, vol. 57, no. 4, pp. 1726–1746, Aug. 2010.

[16] R. A. Reed, R. A. Weller, M. H. Mendenhall, D. M. Fleetwood, K. M. Warren, B. D. Sierawski, M. P. King, R. D. Schrimpf, and E. C. Auden, "Physical Processes and Applications of the Monte Carlo Radiative Energy Deposition (MRED) Code," *Accepted for publication in the IEEE Trans. Nucl. Sci.*, 2015.

[17] J. F. Zeigler and J. P. Biersack, "Stopping and Range of Ions in Matter." [Online]. Available: http://www.srim.org.

[18] N. A. Dodds, M. J. Martinez, P. E. Dodd, M. R. Shaneyfelt, F. W. Sexton, J. D. Black, D. S. Lee, S. E. Swanson, B. L. Bhuva, K. M. Warren, R. A. Reed, J. Trippe, B. D. Sierawski, R. A. Weller, N. Mahatme, N. J. Gaspard, T. Assis, R. Austin, L. W. Massengill, G. Swift, M. Wirthlin, M. Cannon, R. Liu, L. Chen, A. T. Kelly, P. W. Marshall, M. Trinczek, E. W. Blackmore, S.-J. Wen, R. Wong, B. Narasimham, J. A. Pellish, and H. Puchner, "The contribution of low-energy protons to the total on-orbit SEU rate," *Accepted to NSREC 2015*.

[19] J. R. Schwank, M. R. Shaneyfelt, P. E. Dodd, D. McMorrow, J. H. Warner, V. Ferlet-Cavrois, P. M. Gouker, J. S. Melinger, J. A. Pellish, K. P. Rodbell, D. F. Heidel, P. W. Marshall, K. A. LaBel, and S. E. Swanson, "Comparison of Single and Two-Photon Absorption for Laser Characterization of Single-Event Upsets in SOI SRAMs," *IEEE Trans. Nucl. Sci.*, vol. 58, no. 6, pp. 2968–2975, Dec. 2011.

[20] H. H. K. Tang, C. E. Murray, G. Fiorenza, K. P. Rodbell, and M. S. Gordon, "Importance of BEOL Modeling in Single Event Effect Analysis," *IEEE Trans. Nucl. Sci.*, vol. 54, no. 6, pp. 2162–2167, Dec. 2007.

[21] N. Seifert, B. Gill, J. A. Pellish, P. W. Marshall, and K. A. LaBel, "The Susceptibility of 45 and 32 nm Bulk CMOS Latches to Low-Energy Protons," *IEEE Trans. Nucl. Sci.*, vol. 58, no. 6, pp. 2711–2718, Dec. 2011.